Protoplasma (2016) 253:517–530
DOI 10.1007/s00709-015-0830-5

ORIGINAL ARTICLE

Biogenesis of protein bodies during legumin accumulation in developing olive (*Olea europaea* L.) seed

Jose C. Jimenez-Lopez[1,2] · **Agnieszka Zienkiewicz**[2,3,4] · **Krzysztof Zienkiewicz**[2,5] · **Juan D. Alché**[2] · **Maria I. Rodríguez-García**[2]

Received: 22 November 2014 / Accepted: 7 May 2015 / Published online: 21 May 2015

Abstract Much of our current knowledge about seed development and differentiation regarding reserves synthesis and accumulation come from monocot (cereals) plants. Studies in dicotyledonous seeds differentiation are limited to a few species and in oleaginous species are even scarcer despite their agronomic and economic importance. We examined the changes accompanying the differentiation of olive endosperm and cotyledon with a focus on protein bodies (PBs) biogenesis during legumin protein synthesis and accumulation, with the aim of getting insights and a better understanding of the PBs' formation process. Cotyledon and endosperm undergo differentiation during seed development, where an asynchronous time-course of protein synthesis, accumulation, and differential PB formation patterns was found in both tissues. At the end of seed maturation, a broad population of PBs, particularly in cotyledon cells, was distinguishable in terms of number per cell and morphometric and cytochemical features. Olive seed development is a tissue-dependent process characterized by differential rates of legumin accumulation and PB formation in the main tissues integrating seed. One of the main features of the impressive differentiation process is the specific formation of a broad group of PBs, particularly in cotyledon cells, which might depend on selective accumulation and packaging of proteins and specific polypeptides into PBs. The nature and availability of the major components detected in the PBs of olive seed are key parameters in order to consider the potential use of this material as a suitable source of carbon and nitrogen for animal or even human use.

Keywords Cotyledon · Development · Endosperm · Legumin · Protein body · Seed

Handling Editor: Alexander Schulz

Jose C. Jimenez-Lopez and Agnieszka Zienkiewicz contributed equally to this work.

Electronic supplementary material The online version of this article (doi:10.1007/s00709-015-0830-5) contains supplementary material, which is available to authorized users.

✉ Jose C. Jimenez-Lopez
jcjimenezl75@gmail.com; jose.jimenez-lopez@uwa.edu.au

✉ Maria I. Rodríguez-García
mariaisabel.rodriguez@eez.csic.es

[1] The UWA Institute of Agriculture, The University of Western Australia, 35 Stirling Highway, Crawley, Perth, WA 6009, Australia

[2] Department of Biochemistry, Cell and Molecular Biology of Plants, Estación Experimental del Zaidín, National Council for Scientific Research (CSIC), Profesor Albareda 1, Granada 18008, Spain

[3] Department of Plant Physiology and Biotechnology, Nicolaus Copernicus University, Toruń 87-100, Poland

[4] Centre for Modern Interdisciplinary Technologies, Nicolaus Copernicus University, Toruń 87-100, Poland

[5] Department of Cell Biology, Nicolaus Copernicus University, Toruń 87-100, Poland

Introduction

Seed development is a complex and highly coordinated process that conceptually can be divided in a discontinuous, stepwise process where several different phases occur in progression. This physiological process requires the integration of many genetic, physiological, metabolic, and signaling pathways, and it is also affected by endogenous and environmental signals and stimuli (Sabelli et al. 2012). These progressive phases consist in (1) *plant embryogenesis*, where a proper histological differentiation and morphogenesis of viable embryo goes along with rapid cell divisions and polarity acquisition, establishing the root and shoot apical meristems and

bilateral symmetry; (2) *embryo maturation phase*, with the differentiation of specialized storage cells becoming biosynthetically highly active, accumulating huge amounts of storage compounds, and expanding in volume considerably; (3) *desiccation phase*, when the seeds are physiologically mature and the embryo has become tolerant to desiccation, shutting down metabolic activityand entering into dormancy that prevents germination for a period of time (Raissig et al. 2011).

The whole developmental process is characterized by an extensive cross-talk between filial (i.e., embryo) and maternal (i.e., endosperm) tissues, which makes possible a high degree of coordination between seed tissues for a fine regulation of their development (Sreenivasulu et al. 2013).

Seed storage reserves accumulate in compartmentalized structures. During seed development and maturation, proteins are targeted to specialized vacuoles termed as protein bodies (PBs) (Baud et al. 2008). This physiological process is of crucial importance for the successful sexual reproduction of angiosperms since after a variable desiccation period, during seed germination, these macromolecular reserves support the germination process, seedling growth, and plant development (Müntz et al. 2001). Given that seeds are not photosynthetically active, their storage reserves are in great demand at the early stage of seedling growth and plant development (Borisjuk et al. 2004). Thus, nutrients and energy requirements to sustain cell proliferation and tissue growth have to be provided by other tissues, mainly from storage cells of the embryonary axis (Borisjuk et al. 2013). Endosperm is the nursing tissue that has long been known to provide nutrients to the developing embryo (Pignocchi et al. 2009), supporting also seedling development during and after germination in some species (Sabelli et al. 2009). Moreover, endosperm has a morphogenetic role in regulation of embryo development since it has a key role in integrating different signals and cross-talk among the major seed compartments, as well as great influence in the epigenetic mechanisms controlling seed development (Dekkers et al. 2013).

Carbohydrates and proteins are the two major classes of storage compounds. However, seeds also accumulate other important types of reserves, such as lipids stored in oil bodies (OBs), phosphate, minerals, and protease inhibitors that accumulate at differential time frame (Gallardo et al. 2003, 2007). Seed storage proteins (SSPs) have best been characterized mainly in the *Poaceae* family among monocots and in legumes among dicots (Raissig et al. 2011). SSPs have been classified regarding their molecular masses expressed as sedimentation coefficients (*S*) (Shewry et al. 1995) or on basis of their solubility properties. Albumins are soluble in water, globulins in dilute salt solutions, prolamins in alcohol, and glutelins in diluted acids or bases (Osborne et al. 1924).

SSPs in dicotyledonous plants are constituted mainly by the 11S group (or legumin, 11-13S-type globulins), and the 7S group (or vicilin-like, 7-8S-type globulins) of proteins. However, the relative proportions of 7S and 11S globulins can vary widely among different species and even within species (Shewry et al. 2002). These two groups share no obvious sequence similarity, but they form similar holoprotein structures and have a common evolutionary origin (Shutov et al. 2003). The globulins, the most widely distributed group of storage proteins, are part of the Cupin Superfamily and evolved from bacterial enzymes (Dunwell et al. 2004), being 11S-type the most abundant SSPs in dicotyledonous plant species (including legumes), corresponding to 70 % of the total seed nitrogen (Shewry et al. 1995).

Olive endosperm and cotyledon accumulate vast amounts of 11S-type globulins. These types of globulins are hexameric proteins, which are synthesized by two precursor forms, made up of five individual proteins named p1–p5 (20.5, 21.5, 25.5, 27.5, and 30 kDa, respectively), having p1 and p2 basic character, and p3, p4, and p5 acidic character. 11S-type storage proteins are highly soluble in diluted saline solutions (Alché et al. 2006).

SSPs in mature olive seeds accumulate in dense bodies encased by a membrane and named protein bodies (Herman and Larkins 1999). While this feature is common to monocots and dicots, different pathways determine their intracellular trafficking and targeting (Müntz 1998), which not yet investigated in olive seed tissues. Overall, SSPs are synthesized in the rough ER and co-translationally targeted to the ER lumen. Inside the ER lumen, they undergo a number of modifications, i.e., cleavage of the signal peptide, folding, the formation of disulfide bonds, and making multimer forms through non-covalent bonds. The 7S- and 11S-type globulins are targeted through the ER and the Golgi apparatus to specialized storage vacuoles (Herman and Schmidt 2004), often undergoing further processing to form intravacuolar dense bodies. Thus, PBs may eventually result from the division of the vacuoles during seed development and maturation process (Herman and Larkins 1999).

Olive tree is the most extensive and important crop in Mediterranean countries, together with cereals, and one of the sixth most important cultivated plant across the world. Regardless of these facts, seed developmental and maturation processes remain largely unknown.

Our group has previously studied the cytological events accompanying PBs degradation during olive seed in vitro germination and seedling growth (Zienkiewicz et al. 2011a), but no study has been performed so far for the analysis of PB biogenesis despite the importance of PBs as specialized storage cell compartments during olive seed development.

In the present work, we have studied the changes taking place at different developmental and differentiation stages in olive seed storage tissues, endosperm and cotyledon, with a focus on PB formation toward a better understanding of the physiological process underlying storage (legumin) protein accumulation.

Materials and methods

Plant material

Seeds at different developmental stages were obtained from the olive (*Olea europaea* L.) trees cv. Picual grown in the "Estación Experimental del Zaidín", Granada (Spain), taking anthesis as the initial point to the mature seed stage (201 days after anthesis— DAA).

Total protein extraction

Whole seeds, as well as isolated endosperm and cotyledon (0.1 g of each sample), were homogenized separately in a mortar cooled on ice using an extraction buffer (125 mM Tris-HCl (pH 6.8), 0.2 % (*w*/*v*) SDS, 1 % 2-mercapthoethanol). Samples were centrifuged at 13,500 rpm for 30 min at 4 °C, and the resulting supernatants were boiled for 3 min and centrifuged again. Proteins in the supernatants were precipitated with 2 volumes of cold acetone and re-solubilized in extraction buffer. Protein content in each extract was measured by using a commercial Bradford procedure (Bio-Rad).

SDS-PAGE and immunoblotting

Total proteins (25 μg per sample) were separated by SDS-PAGE on CriterionXT Precast Gel (Bio-Rad, USA) using Criterion™ Cell apparatus (Bio-Rad). After electrophoresis gel separation, proteins were stained with Coomassie Brilliant Blue according to standard procedure. Proteins were electroblotted onto a PVDF membrane using Trans-Blot® Turbo™ Transfer Pack (Bio-Rad) in a Trans-Blot®Turbo™ Transfer System (Bio-Rad). The membrane was blocked for 1 h in solution containing 1 % (*w*/*v*) non-fat dry milk in Tris-buffered saline (TBS) buffer, pH 7.4. Immunodetection of legumin proteins was carried out by incubation with rabbit polyclonal antibody (Ab) raised against p1-purified protein (Alché et al. 2006) diluted 1:500 in TBS buffer containing 1 % (*w*/*v*) non-fat dry milk. A DyLight 488 conjugated anti-rabbit IgG (Agrisera), diluted 1:2000 in TBS buffer for 2 h, served as the secondary antibody. The signal was detected in a Pharos FX molecular imager (Bio-Rad). Quantitative analysis of legumin protein (p1–p5) bands in immunoblot images was performed using Quantity One 1-D Analysis Software (Bio-Rad).

Microscopy sample preparation

Cotyledon and endosperm were dissected out from different stages of development of olive seeds from the olive cv. Picual and individually processed for light and transmission electron microscopy. Samples were fixed for 24 h at 4 °C with a mix of 4 % (*w*/*v*) paraformaldehyde and 0.2 % (v/v) glutaraldehyde in 0.1 M cacodylate buffer (pH 7.2). Samples were then dehydrated throughout an ethanol series and embedded in Unicryl resin (BBInternational, UK). After ultraviolet light polymerization of samples at −20 °C for 48 h, both semi-thin (1 μm) and ultra-thin sections (70 nm) were obtained using a Reichert-Jung Ultracut E microtome (Leica Microsystems, Germany). Semi-thin sections were placed on BioBond™ (BBInternational)-coated slides. Ultra-thin sections were mounted on formwar-coated 200-mesh nickel grids.

Seed tissue cytochemistry

For general sample observations, sections were stained with a mixture of 0.05 % (*w*/*v*) methylene blue and 0.05 % (*w*/*v*) toluidine blue (Zienkiewicz et al. 2011a). For protein staining and visualization, sections were stained with a solution consisting in 0.25 % (*w*/*v*) Coomassie Brilliant Blue R-250 and 0.05 % (*w*/*v*) Coomassie Brilliant Blue G-250 dye in a solution of methanol/acetic acid/water (5:1:4). The sections were stained for 5 min at room temperature and washed in running water for 2 min (Fisher 1968).

For carbohydrates and starch granule identification, periodic acid–Schiff (PAS) staining system (Sigma) was used (Parker 1965). The slides were immersed in 1 % (*w*/*v*) periodic acid for 5 min, rinsed in running water for 5 min, and stained in Schiff's reagent for 15 min in the dark, followed by incubation with hematoxylin solution for 2 min.

Sudan Black B was used for staining neutral lipids (Bronner 1975). Sections were stained at 60 °C for 30 min using a saturated solution of Sudan Black B, prepared in 70 % (v/v) ethanol. Observations of samples were carried out with an Axioplan microscope (Carl Zeiss, Germany), and images were recorded with a ProGres C3 digital camera using the ProGresCapturePro v2.6 software (Jenoptik AG, Germany).

Nile red was used to selectively fluorescent stain intracellular lipid droplets to study intracellular OBs formation (Greenspan et al. 1985). Samples were incubated for 10 min in a solution containing 0.05 mg ml^{-1} Nile Red (Sigma-Aldrich) dissolved in acetone. Samples were observed with a Nikon C1 confocal laser scanning microscope (Nikon, Japan) using an argon (488) laser. Z-series images were collected and processed with the software EZ-C1 Gold version 2.10 build 240 (Nikon).

Immunofluorescence analysis of legumin proteins

Immunofluorescence-based cytochemistry was carried out in semi-thin sections (≈1 μm) through a sequential treatment with incubation in blocking solution containing 1 % (*w*/*v*) bovine serum albumin (BSA) in phosphate buffered saline (PBS) solution (pH 7.2), followed by washing steps in PBS (3×15 min each) and incubation overnight at 4 °C with an anti-11S antibody (diluted 1:500) (p1 antiserum raised in

rabbits), additional washing steps in PBS (3×15 min each), and incubation with secondary anti-rabbit IgG DyLight 488-conjugated antibody (Agrisera, Sweden) (diluted 1:250 in blocking solution) for 1 h at 37 °C. In control sections, the primary Ab was omitted. Samples were maintained with an anti-fading (Citifluor/glycerol/PBS, Sigma) agent. The sections were observed and analyzed by using an epifluorescence Zeiss Axioplan microscope (Carl Zeiss, Germany). Images were obtained with a ProGres C3 digital camera using the ProGresCapturePro 2.6 software (Jenoptik AG, Germany).

For immunogold experiments, ultra-thin sections were treated with a blocking solution (5 % (*w*/*v*) (BSA), 0.1 % (v/v) Tween-20 in PBS), a diluted (1:500) solution of the p1 antiserum in blocking solution, and a 1:1000 secondary antibody (goat anti-rabbit IgG/15 nm gold (BBInternational)) solution, and finally samples were contrasted using a 5 % (*w*/*v*) uranyl acetate solution for 30 min at room temperature. Observations were carried out with a JEM-1011 transmission electron microscope (JEOL, Japan). Control reactions were carried out by omitting the primary Ab.

Statistical analyses were performed using SPSS software (version 14.0; SPSS). Student's *t* test was used to compare means of gold grain counts in PBs from endosperm and cotyledon TEM immunogold images compared to controls, as well as densitometry values of proteins detection in immunoblots.

Sample processing for scanning electron microscopy

Initial fixation and dehydration of seed tissues was carried out as described for TEM. After dehydration, samples were critically point-dried using liquid CO_2 as the transition fluid, using a SEM Polaron CPD 7501 critical point dryer (Quorum Technologies Ltd., UK). They were mounted on brass discs with double stick tape and silver cement to ensure a conduction path from the specimen to the stub, coated with gold palladium (20:80) in a PolaronE5000 sputter coater, and observed with a GEMINI (FESEM) Carl Zeiss SMT at 25 kV. Micrographs were collected using secondary electron imaging and back-scattered electron imaging in topographical and compositional modes.

Results

We have studied the time course of seed development until its complete maturation. Figures 1, 2, 3, 4, 5, and 6 show the differentiation steps of olive seed development, from the flower anthesis as starting time until the mature stage of the seed (210 DAA). Seed development was accompanied by visual morphological changes in olive fruit, the color of which changed from green to deep purple as a result of the mesocarp maturation.

Cytochemical analysis of developing endosperm and cotyledon

At the early stages of a fertilized ovule (20DAA) (Figs. 1 and 2), the integuments are around the embryo sac and the nucellus (or nucellus rests). The embryo sac contains the embryo proper in different stages surrounded by cellular endosperm (Fig. 1a). In this endosperm, nucleus divides without wall formation as observed in the magnification detail of Fig. 1a, and in Fig. 1b where nuclei were detected by DAPI. Proteins stained with CBB were detected in the whole cytoplasm, and particularly intensely stained the marginal area of the cytoplasm, since a central vacuole appears in the central cell and pushes the cytoplasm containing the nuclei to the periphery. PAS staining showed the presence of polysaccharides in the cytoplasm (Fig. 1c), and differential staining showed the distribution of storage lipids (Fig. 1d, Sudan Black B, and Fig. 1e, Nile Red). Small vesicles composed of neutral lipids (Fig. 1d) were located in the cytoplasm, well visible as numerous red-orange fluorescence spots in fixed seed material (Fig. 1e). Oil materials enclosed by membranous systems to form OBs were observed at TEM, showing the cytoplasm filling up with electron-transparent bodies of 3 μm in diameter, surrounded by electron-dense membrane (Fig. 1f).

At 60 DAA, it was possible to differentiate an immature embryo from the endosperm in the olive seed. The cytoplasm of endosperm and cotyledon cells was intensely stained with CBB (Figs. 2—B1 and 3—B1), which may reflect the intensification of metabolic activity and protein synthesis/accumulation at this stage. OBs and PBs were more abundant in endosperm cells (Fig. 2—A1) in comparison to cotyledon (Fig. 3—A1). Neutral lipids filled up most of the endosperm cell cytoplasm (Fig. 2—A1 and C1); meanwhile, in the cotyledon cells, OBs mainly lined the plasma membrane (Fig. 3—A1 and C1). In the endosperm cells, proteins were detected in the cytoplasm and accumulated in areas of emerging PBs (Fig. 2—B1), while largely remaining in the cytoplasm of cotyledon cells (Fig. 3—B1).

At a more advanced stage of olive seed development (90 DAA), the cytoplasm in endosperm and cotyledon was full of multiple vacuoles (Figs. 2—B2 and 3—B2), where PBs started to be distinguishable, which were more homogeneously stained in the endosperm. Endosperm cells contained vacuoles filled up with proteins and surrounded by OBs (Figs. 2—B1 and B3 and 3—B1 and B3). Advanced seed maturation states showed protein compartmentalization inside of vacuoles to finally differentiate to PBs (compare Fig. 3—B3 and B4). This could be a characteristic differential feature between endosperm and cotyledon. Both types of tissue showed significant levels of neutral lipid staining in the cytoplasm surrounding PBs, being more intensely stained in the endosperm compared to cotyledon (Figs. 2—A2 and 3—A2).

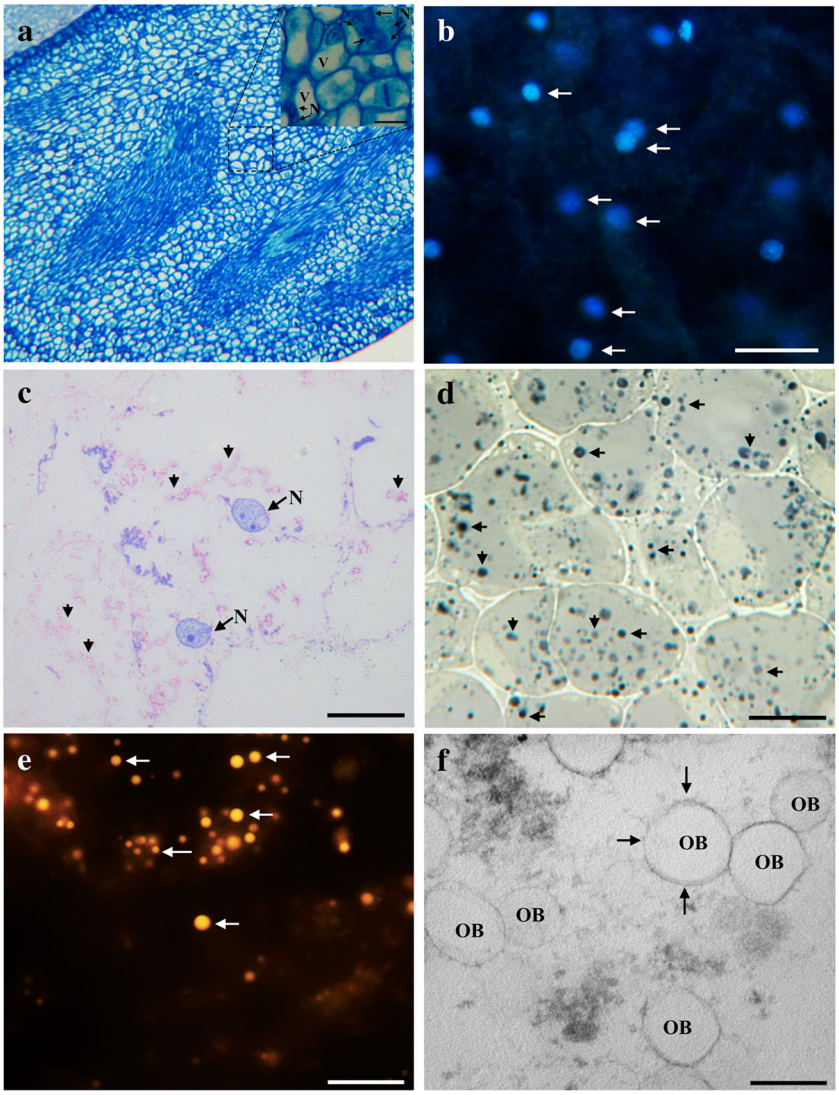

Fig. 1 Histological and cytochemical analysis of olive seed embryo sac tissues at early developmental stage. **a** Olive seed at 20 DAA in longitudinal section stained with toluidine blue. A detailed view of a small region of interest is located inside of this section; *bar*=20 μm. **b** DAPI staining showed nuclei fluorescence highlighted with *arrows; bar*=20 μm. **c** Section stained with Coomassie Brilliant Blue (CBB; *blue*) and PAS (*pink*). Polysaccharides (*pink*) are indicated with *arrows*; *bar*=20 μm. **d** Section stained with Sudan Black B, showing lipids inside small vesicles (*arrows*) in the cytoplasm; *bar*=20 μm. **e** Fluorescence from Nile Red staining perfectly shaped OBs (*arrows*), revealing their lipidic nature; *bar*=10 μm. **f** TEM micrograph of the olive seed cells. OBs with visible membrane (*arrows*) are localized in the cytoplasm; *bar*=3 μm. *N* nuclei, *V* vacuole

At 145 DAA, both endosperm (Fig. 2—ABC3) and cotyledon (Fig. 3—ABC3) cells showed multiple PBs in the cytoplasm surrounded by small lipid vesicles (Figs. 2—B3 and 3—B3), where the endosperm exhibited higher number of PBs homogeneous in electro-density (Fig. 2—C3) compared to the cotyledon (Fig. 3—C3) where PBs had bigger size and exhibited differential electro-density. Furthermore, cotyledon's OBs were loosely distributed around the PBs in comparison to endosperm. PAS staining was visible in both endosperm and cotyledon, mainly staining polysaccharides of the cell walls from 90 DAA onwards (Figs. 2—B2–B4 and 3—B2–B4).

Characteristics features of mature endosperm and cotyledon

The mature stage of olive seed was clearly distinguishable from previous developmental stages since the olive fruit was changed completely into black color, and mesocarp cells were full of oil. The mature olive seed consisted of a brown coat and a relatively thick layer of white endosperm surrounding the embryo. Endosperm and embryo were clearly distinguishable, where embryo exhibited two cotyledons and a radicle.

At 210 DAA, the major morphological differences, as well as cellular distribution of different macromolecular components (proteins, lipids, carbohydrates) in endosperm and cotyledon cells (Figs. 2—A4–C4 and 3—A4–C4, respectively), PBs and OBs in endosperm and cotyledon cells (Figs. 2—A4 to C4 and 3—A4 to C4, respectively) were occupying most of the cytoplasm, and OBs were found as directly surrounding PBs (Figs. 2—A4 and 3—A4). Unlike in endosperm, however, the cotyledon OBs were less numerous and more tightly packed in the cytoplasm. Analysis of endosperm PBs revealed their similar size (between 15 and 25 μm of diameter) and intense and homogeneous CCB staining (Fig. 2—B4). In turn, cotyledon PBs showed significant differences in both size (between 20 and 45 μm of diameter) and CBB staining distribution. These variations were observed not only among the cell population but even in the same cell (Fig. 3—B4).

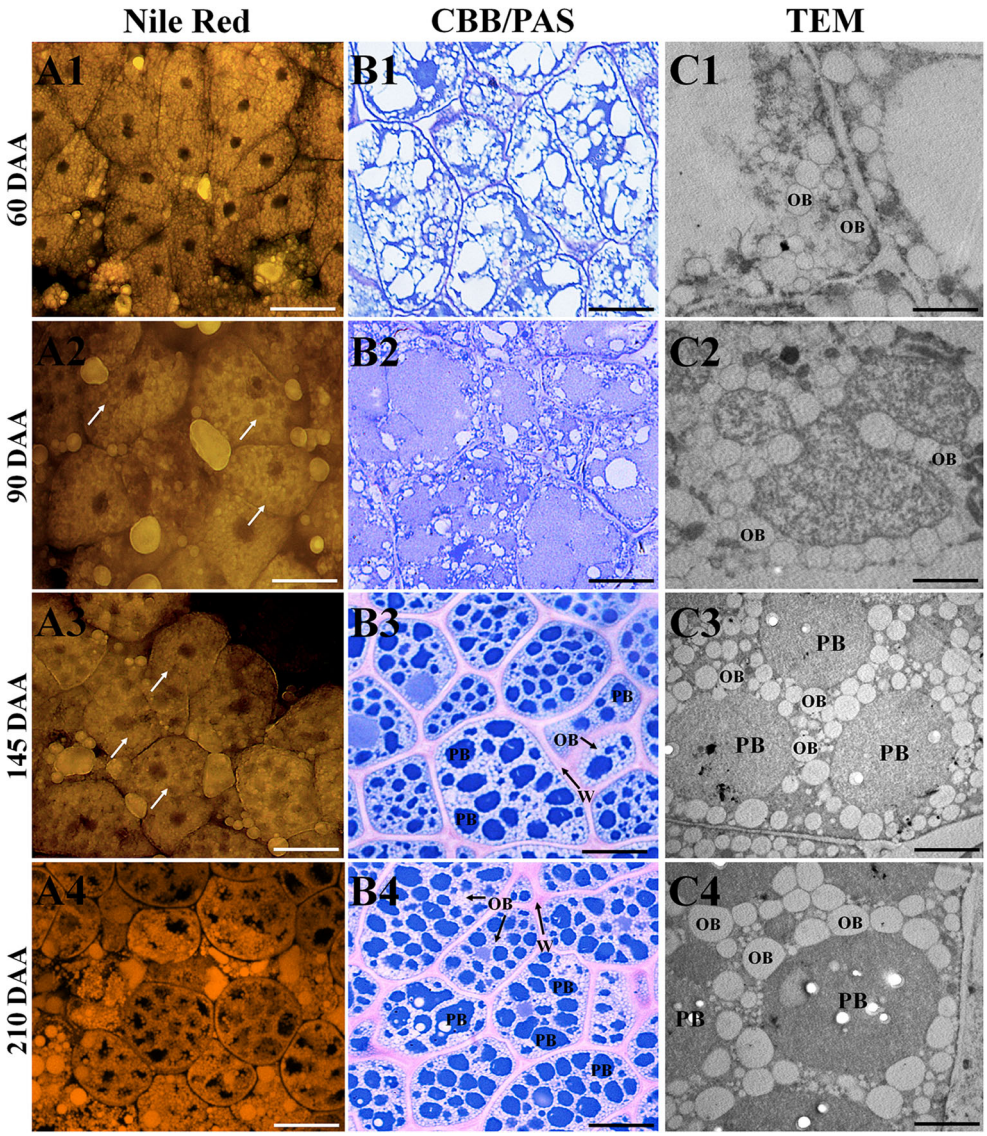

Fig. 2 Cytochemical and ultrastructural study of the endosperm cells during seed development. *A1–A4* localization of OBs by confocal laser scanning microscopy in endosperm cells stained with Nile Red. Numerous OBs are indicated with *arrows*; *bars*=20 μm. *B1–B4* total proteins blue staining (CBB) and pink staining (PAS) cell wall material in endosperm sections; *bars*=20 μm. *C1–C4* TEM micrographs of the endosperm cells; *bars* = 10 μm. *PB* protein body, *OB* oil body

A broad and faint polysaccharide cytoplasmic staining was found after using PAS in both endosperm and cotyledon, but more intense staining was found in cell walls (Figs. 2—B4 and 3—B4), particularly in endosperm cells.

SEM analysis of mature endosperm and cotyledon

Scanning electron micrographs showed evidences of the architectural differences between seed tissues at mature stage (Fig. 4).

Images of the fractured inner layers of the endosperm (Fig. 4a) showed intact cells with polygonal shape, as well as a broken cell with lipid vesicles attached to the cell fractures close to the cell wall. Detailed views of these broken cells (Fig. 4b) allowed appreciation of cell wall architecture and spatial disposition of PBs and OBs inside the cells, as well as fragments of the inter-vesicular cytoplasm matrix, with a beehive-like structure supporting and maintaining the connected cellular OBs and PBs network.

Furthermore, an aggregate of several OBs has been conserved in one of the fracture surface cells (Fig. 4c).

Cotyledon cells showed a comparable structure to endosperm. Elongated palisade parenchyma cells with rectangle shape were distinguishable from the more rounded spongy parenchymatous cells of the sub-apical and central regions of cotyledon (Fig. 4d). A detailed view of the rounded spongy parenchymatous cells (Fig. 4e) showed the spatial distribution of PBs and OBs inside the cells, with the contours of PBs imprinted in the cytoplasm matrix, showing the localization of OBs surrounding PBs. Aggregated structures composed of several OBs have been conserved in few of the cells in the fracture in intact distribution in the cell, as well as the material connecting these vesicles (Fig. 4f).

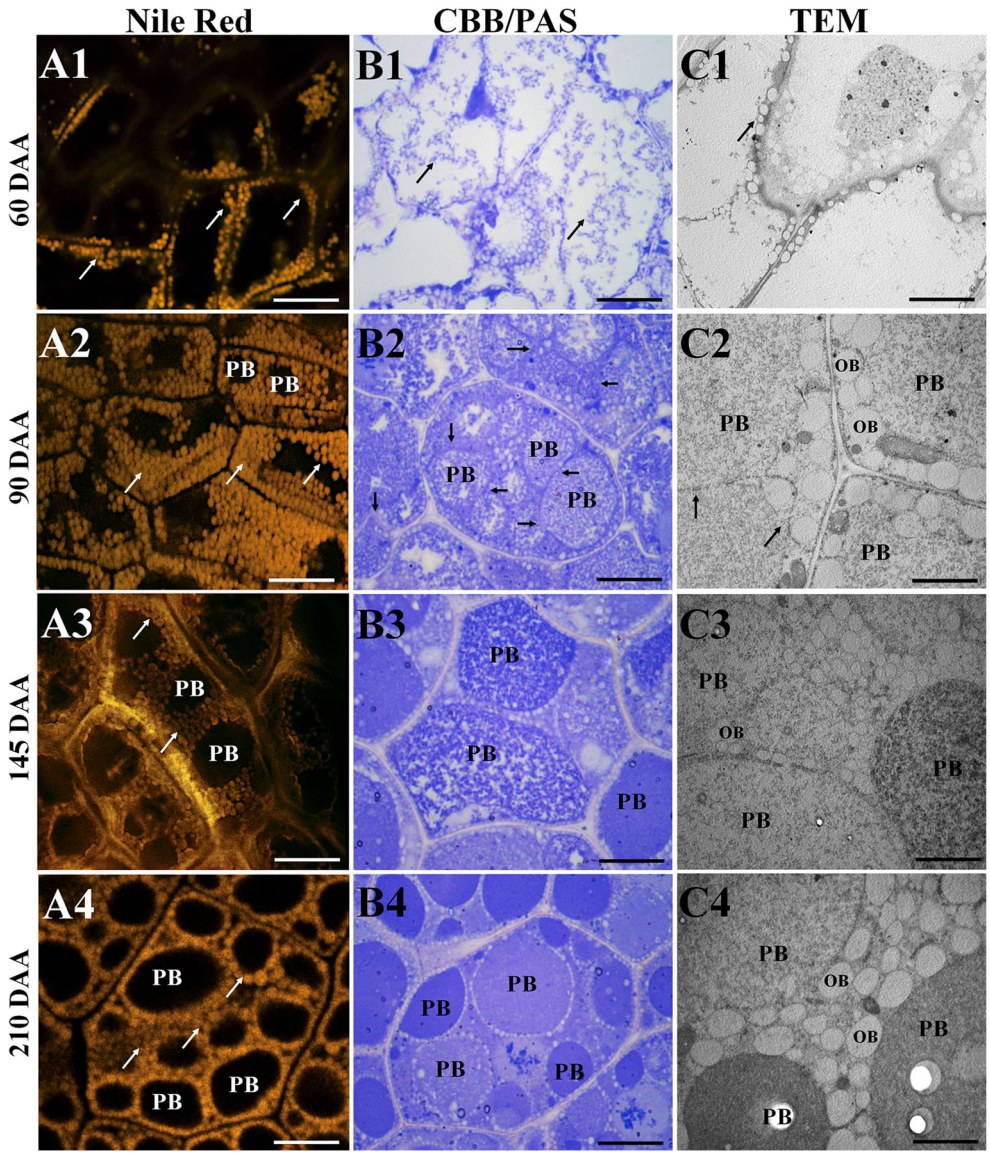

Fig. 3 Cytochemical and ultrastructural study of the cotyledon cells during seed development. *A1–A4* localization of OBs by confocal laser scanning microscopy in cotyledon cells stained with Nile Red. Numerous OBs are indicated with *arrows*; *bars*=10 μm. *B1–B4* total proteins blue staining (CBB) and pink staining (PAS) cell wall material in cotyledon sections; *bars*=20 μm. *C1–C4* TEM micrographs of the cotyledon cells; *bars*=10 μm. *PB* protein body, *OB* oil body

Legumin protein synthesis during seed development

In order to analyze the time-course of SSP synthesis and compare it with cytochemical observations at different developmental stages of the endosperm and cotyledon, we performed protein extractions at the different developmental stages to detect legumin proteins by immunoblot assays (Fig. 5a). The legumin levels significantly increased during seed development. Immunoblot experiments showed the presence of five bands (p1–p5) representing the reduced components of legumin proteins, which were cross-recognized by the p1-antiserum. The specificity of this antibody was demonstrated previously (Alché et al. 2006). The protein bands were observed in all analyzed stages after the immunoblot reactions. An initial synthesis of legumin proteins was distinguishable when whole seeds were analyzed at 20 DAA and continued with massive synthesis levels at 60 DAA as it was indicated in endosperm, reaching the highest levels in mature seed stage (210 DAA). Alternatively, low amount of protein was immuno-detected at 60 DAA in cotyledon, but a massive synthesis was noticeable from 90 DAA. From this stage until 145 DAA, comparable levels of legumin proteins were immuno-detected in cotyledon and endosperm tissues (Fig. 5a).

Quantitative analysis of legumin protein (p1–p5 peptides) bands (Fig. 5b) has shown comparable densitometric profiles in both seed tissues (cotyledon and endosperm) from 90 to 210 DAA, without statistically significant differences ($p>0.05$). Furthermore, the plot showed an increased tendency in protein quantity, more pronounced in cotyledon compared to endosperm and a comparable (highest) peak at seed mature stage. However, appreciable statistical differences ($p<0.05$) have been found in the level of proteins at 60 DAA.

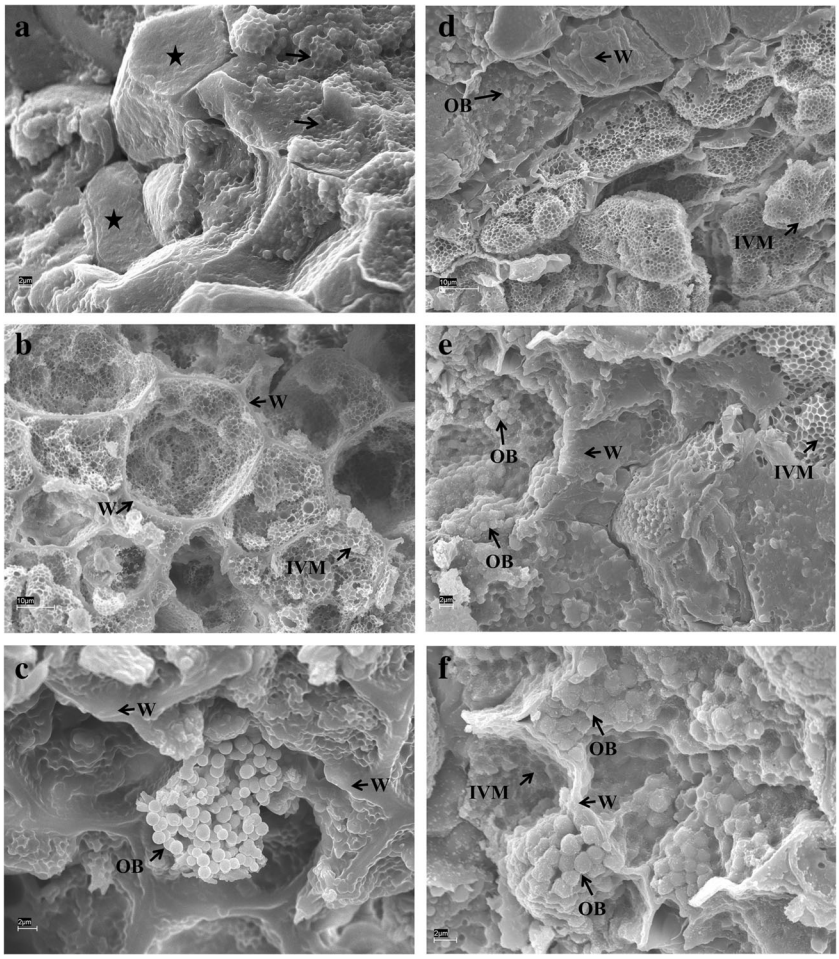

Fig. 4 Scanning electron microscopy analysis of mature endosperm and cotyledon. **a** View of endosperm complete and broken cells, showing the disposition of OBs; *bar*=2 μm. **b** Detailed view of the fracture surface, where particularly are appreciated the spatial disposition and contours of PBs and OBs based in their fingerprints; *bar*=10 μm. **c** Detailed view of OBs aggregate in an endosperm cell. Some degree of OB coalescence is appreciated in the cells, a phenomenon which may be probably correlated with the reduced amount (extraction) of oil-body associated proteins in the endosperm; *bar*=2 μm. **d** View of the parenchymatous cells in cotyledon. OBs are conserved in the upper layer cells close to the cell wall. Inter-vacuolar material was patent in the lower layers of cells as a beehive-like structure; *bar*=10 μm. **e** OB details connected by inter-vacuolar material. No protein bodies are visible in the surface of the fractured cells; *bar*=2 μm. **f** Detailed view of OBs aggregates; *bar*=2 μm. *IVM* inter-vesicular material, *PB* protein body, *OB* oil body, *W* cell wall

PBs formation during olive seed development

Legumin proteins have been used as molecular biomarker to study the biogenesis of PBs during seed (endosperm and embryo) development and maturation by using immunofluorescence and TEM assays.

At 20 DAA, small proteinaceous accumulations were visible for the first time in seed tissues. They were located in the marginal cytoplasm, around a large central vacuole, corresponding to legumin proteins as it was corroborated by immunofluorescence (Fig. 6—A0) and immunogold (Fig. 6—B0) detection.

From this stage onward, a SSP synthesis and gradual developmental accumulation were observable within the endosperm and cotyledon (Fig. 6). Two different patterns of PB formation were distinguishable in seed tissues—a feature that may differentiate endosperm and cotyledon developmental process, particularly from 90 to 145 DAA.

At 60 DAA, immunofluorescence in both storage tissues appeared diffusely distributed within the cytoplasm. Endosperm cells exhibited increasing protein accumulation in the cytoplasm, but fluorescent and immunogold labeling was markedly detected in areas of emerging PBs (Fig. 6—A1 and A2), while cotyledon cells showed lightly diffuse cytoplasmic fluorescence, with few protein clusters of irregular shape more densely marked by gold grains (Fig. 6—B1 and B2).

At 90 DAA, endosperm cells showed dense cytoplasmic florescence and abundant immunogold labeling, accompanied by the presence of numerous vesicles in formation, characterized by regular and increasing size (Fig. 6—A3 and A4). Cotyledon cells showed a full cytoplasm of diffuse

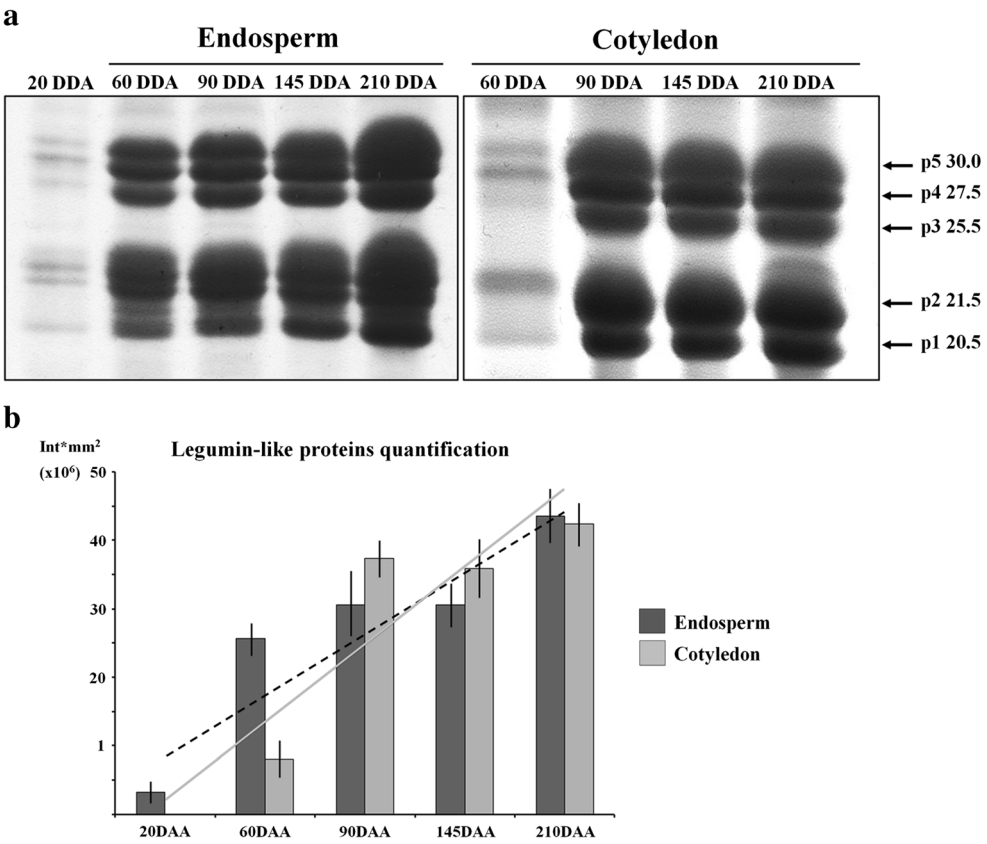

Fig. 5 Immunoblot analysis of legumin proteins during seed development. **a** Immunoblot of total protein extracts obtained from olive endosperm and cotyledon at different stages of development. PVDF membranes transferred with protein extracts were probed with a polyclonal antiserum raised against p1-purified protein (Alché et al. 2006). Different subunits that integrate legumin proteins are highlighted as P1-P5. **b** Quantitative densitometric analysis of legumin proteins (p1-p5 peptides) in immunoblot images by using Quantity One 1-D Analysis Software (Bio-Rad). Tendency (*continuous* and *dashed*) *lines* are plotted for cotyledon and endosperm, respectively

fluorescence, accompanied by the apparition of legumin-rich protein bodies (Fig. 6—B3, arrows). Gold grains were located mainly in the diffuse material of the cytoplasm, but also inside of the forming PBs (Fig. 6—B4). These observations may suggest a two-step PB formation process: (1) in endosperm cells, by increasing size and fluorescence intensity of membranous-evolved bodies; (2) in cotyledon cells, by the accumulation of proteins in the whole cytoplasm followed by further compartmentalization in few large protein bodies after reaching a critical size/mass and proteins.

At 145 DAA, endosperm cells showed small and numerous well-defined PBs, occupying most of the cell area. Proteinaceous material was still being compartmentalized inside PBs. The fluorescence of low intensity was detected in just-emerged PBs (Fig. 6—A5) and gold grains were almost exclusively detecting proteins inside of PBs (Fig. 6—A6). Beside legumin proteins accumulated in PBs, diffuse cytoplasmic signal was still visible in both types of tissue, particularly more abundant in cotyledon cells. Intensively labelled and well-defined PBs, as well as a rich pool of proteinaceous material distributed in the cytoplasm, were distinguishable at this stage in cotyledon cells (Fig. 6—B5). This pattern was confirmed at TEM level by abundant immunogold labeling of defined PBs (Fig. 6—B6).

At mature stage (210 DAA), a homogeneous population of PBs was observed in endosperm cells, with small differences in fluorescence signal intensity (Fig. 6—A7), in addition to a characteristic regular shape and their large number per cell. Immunogold assay showed numerous gold grains in PBs, pointing to the accumulation of SSPs (Fig. 6—A8). On the other hand, large differences in fluorescence intensity were found among PB population in cotyledon cells (Fig. 6—B7). Moreover, a broad range of PBs of different sizes and their variable number per cell were also other main features that distinguished cotyledon cells from endosperm. Cotyledon PBs also showed strong gold labelling (Fig. 6—B8).

Negative controls (omitting P1 antibody) were performed for both, immunofluorescence (Fig. S1a) and immunogold (Fig. S1b) assays for every single stage of the seed development and maturation. In the first case, no fluorescence was detected besides a low level of auto-fluorescence mainly from cell walls in immunofluorescence assays. In addition, significant statistical differences ($p<0.05$) were found in gold grain amounts when compared with negative control immunogold images at TEM (5±2 gold grains) and those from endosperm (448±23 gold grains) or cotyledon (387±34 gold grains).

Discussion

Overall, seed developmental processes in monocot and dicot plants are essentially comparable. These include a

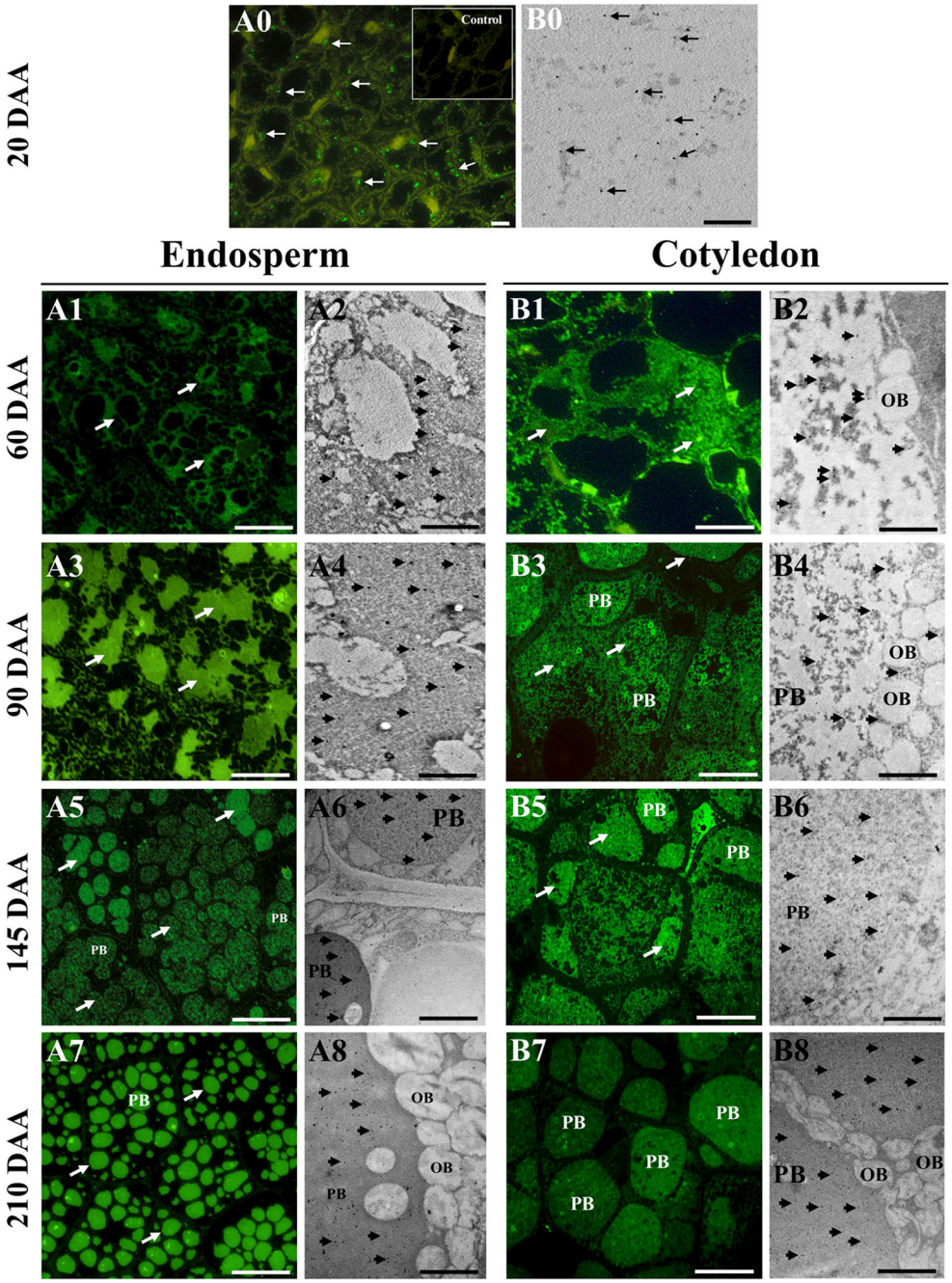

Fig. 6 Localization of legumin proteins in the endosperm and cotyledon cells during seed development. *A0* immunofluorescence localization of legumin protein clusters in the marginal side of the cytoplasm is visible for the first time at 20DAA. *Upper right image* is the negative control (omitting anti-P1 protein–primary antibody) showing only a low level of auto-fluorescence; *bar*=10 μm. *B0* ultrastructural localization of legumin proteins. Gold particles are localized in the cytoplasm (*arrows*); *bar*=5 μm. Immunofluorescence localization of legumin proteins in endosperm (*A1*, *A3*, *A5*, *A7*) and cotyledon (*B1*, *B3*, *B5*, *B7*) tissues. Fluorescent labeling of legumin proteins is located in the cytoplasm (*arrows*). The proteins may accumulate in the ER as consequence of these protein syntheses at a co-translational insertion into the ER's lumen, and further formation of pre-vacuolar compartments either via the Golgi or directly from the ER, and finally storage into large vacuoles. At mature stage, immunofluorescence indicates the presence of legumin proteins mainly inside the PBs; *bars*= 20 μm. Ultrastructural localization of legumin proteins in endosperm (*A2*, *A4*, *A6*, *A8*) and cotyledon (*B2*, *B4*, *B6*, *B8*) tissues. Gold labeling (*arrows*) is present mainly in PB matrix; *bars*=20 μm. *PB* protein body, *OB* oil body

morphogenetic phase characterized by intense cell proliferation, a transition to a phase of accumulation of macromolecules and metabolites that involves a switch from maternal to filial control and a maturation phase characterized by the completion of the storage reserve accumulation. Also, a quiescent state of the embryo is frequently established, where the seed undergoes dehydration (Vicente-Carbajosa and Carbonero 2005). However, the details of seed development vary considerably among different species even within the same taxonomic group (Sreenivasulu and Wobus 2013).

Much of our current knowledge about seed development and maturation processes, including reserve macromolecule synthesis and accumulation, and the regulation of these physiological processes come from monocot seed studies, i.e., cereals (Li et al. 2013). Available information from dicotyledonous seeds focusing into tissue cytochemical and ultrastructural organization is limited to a few species, and this information in oleaginous species is even more scarce (Ferreira Moura et al. 2010).

The current study characterizes different stages of olive seed development at cytological level, revealing specific features and events that define the course of seed physiological changes during its maturation. In addition, our study showed the correlation between key developmental changes occurring

in the olive seed and changes in the structural organization of endosperm and cotyledon cells. Using legumin proteins as a molecular maker, we observed that SSP synthesis and their cytoplasmic accumulation started at 20 DAA, and these data are in accordance with the previous reports on legumin gene family transcript expression in other plant species, i.e., *Medicago truncatula* (Gallardo et al. 2008), *Lupinus angustifolius* (Foley et al. 2011 and 2015). SSP synthesis and accumulation as well as PB formation have been shown to be non-synchronic and tissue-dependent developmental processes. This is reflected in a differential rate of legumin protein synthesis, being more advanced in endosperm, where a high peak of legumin levels was observed at 60 DAA. This massive synthesis increased through the course of seed development. However, cotyledon exhibited a massive peak of SSP synthesis at 90 DAA. In addition, cytochemical observations showed that when PB formation is almost complete in endosperm cells, this tissue exhibited a population of PBs similar in size, while in cotyledon cells only few well-formed PBs were found at that time. This suggests temporal differences in PB formation patterns between two analyzed seed tissues (Abirached-Darmency et al. 2012), occurring slower in cotyledon cells and continued almost until the mature stage. Moreover, PB formation time-course in olive endosperm may be characterized by a more gradual SSP synthesis during seed development, especially from 60 to 210 DAA, as the increase of fluorescence intensity corresponding to the legumin marker was observed in the initial vacuoles, filling up from cytoplasmic proteinaceous content and accompanied by a massive peak of legumin protein level at 60 DAA. Olive cotyledon cells may be characterized also by an accumulation of proteins in the ER distributed in the whole cytoplasm as a consequence of these protein syntheses at a co-translational insertion into the ER's lumen. Further formation of prevacuoles either via the Golgi or directly from the ER would happens, resulting in compartmentalization into large vacuoles (Frigerio et al. 2008). These events were correlated with a delayed peak of legumin synthesis (in comparison to endosperm) observed at 90 DAA and its weak variations until the mature stage of the seed.

The bulk of SSP synthesis and accumulation took place at the early–middle stage of seed development, unlike many other species where synthesis is more intensive at late stages of seed development, constituting a sink of nitrogen (Müntz et al. 2001). Our observations in olive seed tissues point out a different temporal pattern of PB formation when compared with species like *V. faba*, where the main storage phase of protein deposition starts in cotyledon, with a short period of formation of a few, little protein bodies in the embryo proper at early globular stage (Panitz et al. 1995) or with SSP synthesis in *Lathyrus tuberosus* where synthesis starts even earlier (15 DAA) (Knake-Sobkowicz and Marciniak 2005). The patterns of SSP synthesis in olive seem to be similar in turn to the expression profile of seed protein genes in some species (Gallardo et al. 2003, 2007). In *M. truncatula*, this expression rates decline during the late seed maturation period (145 DAA onward) before lipid accumulation is completed (Morton et al. 1995). However, we observed that in olive legumin proteins synthesis continues until mature stage (210 DAA) in both endosperm and cotyledon.

Lipids also accumulate in large quantity in differentiating olive seed tissues. During olive seed development, an increasing population of OBs was observed in endosperm and cotyledon cells. Moreover, the lipid synthesis rates seem to be positively correlated with SSP accumulation. Indeed it was shown that the timing of oleosin, vicilin, and legumin biosynthesis is consistent with a highly coordinated production of both oil and protein bodies in *M. truncatula* seeds (Wang et al. 2012).

At seed maturity, our observations particularly indicated that cellular arrangement of OBs is not random and differs between endosperm and cotyledon cells, which are clearly observed in our characterization of endosperm and cotyledon at SEM. OBs are located around PBs, showing uniformity in size and shape in endosperm, but a broad range of sizes and number of PBs per cell were found in cotyledon cells. Furthermore, in most of the cotyledon cells, OBs surround PBs and line the plasma membrane but are rarely found as free in the cytoplasm. These features may depend on the seed species (Tonnet and Snudden 1974) in addition to a particular physicochemical relationship of OBs with PBs (Djemel et al. 2005; Lott and Buttrose 1978).

A feature that may also characterize the developmental differentiation of olive cotyledon and endosperm processes could be the close interrelationship between PB and OB formation, which may be established in both seed tissues, and where the OB population may be dependent on PB formation, especially in cotyledon cells. This relationship may be highlighted because of the fact that there is a spatial–functional relationship between PBs and several key enzymes (phospholipase A, lipase, and lipoxygenase) involved in storage lipid mobilization from OBs in olive cotyledon cells (Zienkiewicz et al. 2014). OBs in cotyledon cells are gradually formed along with a massive synthesis of proteins from 90 DAA. Meanwhile, lipid and protein synthesis and accumulation seem to be happening in a parallel and progressive fashion in endosperm at 60 DAA.

Time-course and patterns of PB formation are important features that may distinguish the differentiation process in olive endosperm and cotyledon. These developmental features are distinctive of particular seed species and may be largely influenced by the length of period of time when massive storage protein synthesis and accumulation take place (Gallardo et al. 2003, 2007). Furthermore, translation and accumulation of legumin proteins is a highly coordinated process reflected in PB and OB formation, and this coordination also

involves acquiring a characteristic protein/lipid ratio (Wang et al. 2012). The comparison of legumin protein accumulation in endosperm and cotyledon showed that these processes are not accomplished at the same rate (synchronously) in olive (Wang et al. 2013). PB formation in cotyledon cells starts after a massive protein synthesis, when the whole cytoplasm is full of SSPs, and after reaching a critical protein mass, the central vacuole initiates progressive division and compartmentalization, which may promote cytoplasm division and proteins into protein storage vacuoles (PSVs), and further formation of mature PBs (Abirached-Darmency et al. 2012; Hoh et al. 1995). The cytoplasm of cotyledon cells is divided in three to four large vacuoles with different stages of maturation (145 DAA) as a concomitant process with the apparition of PBs, with noticeable differential protein content and size. These differences are more patented in PBs at maturation stage (Jimenez-Lopez and Hernandez-Soriano 2013, 2014). Protein accumulation time-course and PB formation may be strongly influenced by differences in the relative abundance and differential targeting of proteins to vesicles during PB formation as well as might depend on the polypeptide composition of mature SSPs (Herman and Larkins 1999).

At the end of the olive seed developmental process, the cells of endosperm and cotyledon exhibit a cytoplasm full of PBs containing a major amount of legumin proteins (Alché et al. 2006; Zienkiewicz et al. 2011a; Jimenez-Lopez and Hernandez-Soriano 2013, 2014). However, the presence of different populations of these PBs is a major feature that also distinguishes both tissues (Jimenez-Lopez and Hernandez-Soriano 2013, 2014). Olive endosperm and cotyledon cell might be characterized and differentiated by these specific features (Abirached-Darmency et al. 2012) using legumin proteins as biomarker, i.e., cotyledon PB population is distinguishable by noticeable differences in morphometric characteristics, number per cell (about 16 PBs per cell), stainability (CBB), electron density at TEM level, and immunofluorescence labeling for both, PBs inside individual cells and among the whole analyzed population of cotyledon cells. However, PB population among endosperm cells was more homogeneous in terms of the features mentioned above. These cytochemical and morphometric differences between endosperm and cotyledon during PB biogenesis are clearly distinguishable in the mature seed, which might be due to some extension in SSP synthesis, accumulation, and packaging into PB during endosperm and cotyledon differentiation (in Arabidopsis, Shimada et al. 2003; in olive, Jimenez-Lopez and Hernandez-Soriano 2013, 2014). As we suggested previously, this heterogeneity of PBs in size and number per cell may be also the result of a different mechanism at the level of selective accumulation and packaging of mature polypeptides of the SSPs inside the different PBs (Jimenez-Lopez and Hernandez-Soriano 2013, 2014). Additionally, variability of PB populations may also be strongly influenced by the type of cell in these seed storage tissues, SSP synthesis, and transport (targeting) inside PSVs via ER–Golgi and/or direct ER–vacuole pathways, which ultimately depend on the cellular conditions (Herman and Larkins 1999; Müntz 1998).

This study is of great interest in order to assess the potential uses of the olive seed (see the review of Rodriguez et al. 2008), particularly for alimentary purposes. Initial characterization of the digestibility of 11S globulins and PBs (in tissue) has been carried out, and allergenicity has been preliminarily assessed for this material (Zienkiewicz et al. 2011b). This source of protein and oil currently considered as a by-product of olive oil and table olive industries may represent a valuable source of food for animals, and even for human consumption. Therefore, studies as the present one are needed to characterize in detail the raw material, helping to develop industrial, nutritional, productive, and even biotechnological aspects of their use.

In the present study, differential features were observable in both endosperm and cotyledon during developmental differentiation, markedly characterizing this process as (1) tissue specific, including differential rates (asynchronous time-course) of SSP synthesis and accumulation, (2) tissue-dependent patterns of PB formation, and (3) differential populations of PBs in cotyledon cells, clearly distinguishable at mature stage (inside individual cells and between cells), (4) differential morphometric (size and shape) characteristics and tight association of OBs with PBs, particularly in cotyledon cells, which may point out a tight spatio-functional relationship between PBs and OBs.

These differential features significantly emphasize the specific nature and functional and physiological roles that each seed tissue is being developmentally strengthened to drive plant growth and development.

Acknowledgments JCJ-L thanks the Spanish CSIC and the European Research Program Marie Curie (FP7-PEOPLE-2011-IOF) for his I3P-BPDCSIC and PIOF-GA-2011-301550 grants, respectively. AZ and KZ thank the Spanish CSIC for their respective postdoctoral fellowships. The authors would like to thank C. Martinez-Sierra for excellent technical assistance. This study was supported by the following European Regional Development Fund co-financed grants: MCINN BFU 2004-00601/BFI, BFU 2008-00629, BFU2011-22779, CICE (Junta de Andalucía) P2010-CVI15767, P2010-AGR6274, P2011-CVI-7487, and by the European Research Program Marie Curie (FP7-PEOPLE-2011-IOF) to JCJ-L and JDA. The funders had no role in study design, data collection and analysis, decision to publish, or preparation of the manuscript.

Authors' contributions JCJ-L, AZ, JDA, and MIR-G conceived and designed the study. JCJ-L and AZ performed the study. JCJ-L, AZ, KZ, JDA, and MIR-G analyzed, discussed, and assessed the resulting data. JDA and MIR-G contributed reagents/materials/analysis tools. JCJ-L, AZ, KZ, JDA, and MIR-G wrote the paper.

Conflict of interest The authors declare that they have no conflict of interest.

References

Abirached-Darmency M, Dessaint F, Benlicha E, Schneider C (2012) Biogenesis of protein bodies during vicilin accumulation in *Medicago truncatula* immature seeds. BMC Res Notes 5:409

Alché JD, Jimenez-Lopez JC, Wang W, Castro AJ, Rodríguez-García MI (2006) Biochemical characterization and cellular localization of 11S type storage proteins in olive (*Olea europaea* L.) seeds. J Agric Food Chem 54:5562–5570

Baud S., Dubreucq B., Miquel M., Rochat C., Lepiniec L (2008) Storage reserve accumulation in *Arabidopsis*: metabolic and developmental control of seed filling. In: American Society of Plant Biologists (Eds.), The *Arabidopsis* book. e0113

Borisjuk L, Rolletschek H, Radchuk R, Weschke W, Wobus U, Weber H (2004) Seed development and differentiation: a role for metabolic regulation. Plant Biol 6:375–386

Borisjuk L, Neuberger T, Schwender J, Heinzel N, Sunderhaus S, Fuchs J, Hay JO, Tschiersch H, Braun HP, Denolf P, Lambert B, Jakob PM, Rolletschek H (2013) Seed architecture shapes embryo metabolism in oilseed rape. Plant Cell 25:1625–1640

Bronner R (1975) Simultaneous demonstration of lipids and starch in plant tissues. Stain Technol 50:1–4

Dekkers BJ, Pearce S, van Bolderen-Veldkamp RP, Marshall A, Widera P, Gilbert J, Drost HG, Bassel GW, Müller K, King JR, Wood AT, Grosse I, Quint M, Krasnogor N, Leubner-Metzger G, Holdsworth MJ, Bentsink L (2013) Transcriptional dynamics of two seed compartments with opposing roles in Arabidopsis seed germination. Plant Physiol 163(1):205–215

Djemel N, Guedon D, Lechevalier A, Salon C, Miquel M, Prosperi JM, Rochat C, Boutin JP (2005) Development and composition of the seeds of nine genotypes of the *Medicago truncatula* species complex. Plant Physiol Biochem 43:557–566

Dunwell JM, Purvis A, Khuri S (2004) Cupins: the most functionally diverse protein superfamily? Phytochemistry 65:7–17

Ferreira Moura E, ContinVentrella M, YoshimitsuMotoike S (2010) Anatomy, histochemistry and ultrastructure of seed and somatic embryo of *Acrocomia aculeata* (Arecaceae). Sci Agric 67(4):399–407

Fisher DB (1968) Protein staining of ribbonedepon sections for light microscopy. Histochem 16:92–96

Foley RC, Gao LL, Spriggs A, Soo LY, Goggin DE, Smith PM, Atkins CA, Singh KB (2011) Identification and characterization of seed storage protein transcripts from *Lupinus angustifolius*. BMC Plant Biol 11:59

Foley RC, Jimenez-Lopez JC, Kamphuis LG, Hane JK, Melser S, Singh KB (2015) Analysis of conglutin seed storage proteins across lupin species using transcriptomic, protein and comparative genomic approaches. BMC Plant Biol 15:106

Frigerio L, Hinz G, Robinson DG (2008) Multiple vacuoles in plant cells. Rule or exception? Traffic 9:1564–1570

Gallardo K, Le Signor C, Vandekerckhove J, Thompson RD, Burstin J (2003) Proteomics of *Medicago truncatula* seed development establishes the time frame of diverse metabolic processes related to reserve accumulation. Plant Physiol 133:664–682

Gallardo K, Firnhaber C, Zuber H, Héricher D, Belghazi M, Henry C, Küster H, Thompson R (2007) A combined proteome and transcriptome analysis of developing *Medicago truncatula* seeds: evidence for metabolic specialization of maternal and filial tissues. Mol Cell Proteomics 6:2165–2179

Gallardo K, Thompson RD, Burstin J (2008) Reserve accumulation in legume seeds. C R Biol 331:755–762

Greenspan P, Mayer EP, Fowler SD (1985) Nile Red: a selective fluorescent stain for intracellular lipid droplets. J Cell Biol 100:965–973

Herman EM, Larkins BA (1999) Protein storage bodies and vacuoles. Plant Cell 11:601–613

Herman EM, Schmidt M (2004) Endoplasmic reticulum to vacuole trafficking of endoplasmic reticulum bodies provides an alternate pathway for protein transfer to the vacuole. Plant Physiol 136:3440–3446

Hoh B, Hinz G, Jeong BK, Robinson DG (1995) Protein storage vacuoles form de novo during pea cotyledon development. J Cell Sci 108: 299–310

Jimenez-Lopez JC, Hernandez-Soriano MC (2013) Protein bodies in cotyledon cells exhibit differential patterns of legumin-like proteins mobilization during seedling germinating stages. Am J Plant Sci 4: 2444–2454

Jimenez-Lopez JC, Hernandez-Soriano MC (2014) Functional differences of storage proteins are reflected in their mobilization patterns from protein bodies in cotyledon cells during olive (*Olea europaea L.*) seed germination. Commun Agric Appl Biol Sci 79(1):187–192

Knake-Sobkowicz S, Marciniak K (2005) Cellular accumulation of protein bodies and changes in DNA ploidy level during seed development of *Lathyrus tuberosus* L. Acta Biol Cracov Bot 47:147–157

Li M, Lopato S, Kovalchuk N, Langridge P (2013) Functional genomics of seed development in cereals. In: (Ed.), Cereal genomics II. Springer, 215–245

Lott JNA, Buttrose MS (1978) Globoids in protein bodies of legume seed cotyledons. Aust J Plant Physiol 5:89–111

Morton RL, Quiggin D, Higgins TJV (1995) Regulation of seed storage protein gene expression. In: Marcel Dekker (Ed.), Seed development and germination. 103–138

Müntz K (1998) Deposition of storage proteins. Plant Mol Biol 38:77–99

Müntz K, Belozersky MA, Dunaevsky YE, Schlereth A, Tiedemann J (2001) Stored proteinases and the initiation of storage protein mobilization in seeds during germination and seedling growth. J Exp Bot 52:1741–1752

Osborne TB (1924) The vegetable proteins, 2nd edn. Longmans Green, London

Panitz R, Borisjuk L, Manteuffel R, Wobus U (1995) Transient expression of storage-protein genes during early embryogenesis of *Vicia faba*: synthesis and mobilization of vicilin and legumin in the embryo, suspensor and endosperm. Planta 196:765–774

Parker J (1965) Stains for strands in sieve tubes. Stain Technol 40:223–225

Pignocchi C, Minns GE, Nesi N, Koumproglou R, Kitsios G, Benning C, Lloyd CW, Doonan JH, Hills MJ (2009) ENDOSPERM DEFECTIVE1 is a novel microtubule associated protein essential for seed development in Arabidopsis. Plant Cell 21:90–105

Raissig MT, Baroux C, Grossniklaus U (2011) Regulation and flexibility of genomic imprinting during seed development. Plant Cell 23:16–26

Rodríguez G, Lama A, Rodríguez R, Jiménez A, Guillén R, Fernández-Bolaños J (2008) Olive stone an attractive source of bioactive and valuable compounds. Bioresour Technol 99:5261–5269

Sabelli PA (2012) Seed development: a comparative overview on biology of morphology, physiology, and biochemistry between monocot and dicot plants. In: Springer (Eds.), Seed development: OMICS technologies toward improvement of seed quality and crop yield. 3–25

Sabelli PA, Larkins BA (2009) The development of endosperm in grasses. Plant Physiol 149:14–26

Shewry PR, Halford NG (2002) Cereal seed storage proteins: structures, properties and role in grain utilization. J Exp Bot 53:947–958

Shewry PR, Napier JA, Tatham AS (1995) Seed storage proteins: structures and biosynthesis. Plant Cell 7:945–956

Shimada T, Fuji K, Tamura K, Kondo M, Nishimura M, Hara-Nishimura I (2003) Vacuolar sorting receptor for seed storage proteins in *Arabidopsis thaliana*. Proc Natl Acad Sci USA 100:16095–16100

Shutov AD, Bäumlein H, Blattner FR, Müntz K (2003) Storage and mobilization as antagonistic functional constraints on seed storage globulin evolution. J Exp Bot 54:1645–1654

Sreenivasulu N, Wobus U (2013) Seed-development programs: a systems biology-based comparison between dicots and monocots. Annu Rev Plant Biol 64:189–217

Tonnet M, Snudden P (1974) Oil and protein content of the seeds of some pasture legumes. Aust J Agric Res 25:767–774

Vicente-Carbajosa J, Carbonero P (2005) Seed maturation: developing an intrusive phase to accomplish a quiescent state. Int J Dev Biol 49:645–651

Wang XD, Song Y, Sheahan MB, Garg ML, Rose RJ (2012) From embryo sac to oil and protein bodies: embryo development in the model legume *Medicago truncatula*. New Phytol 193:327–338

Wang J, Shen J, Cai Y, Robinson DG, Jiang L (2013) Successful transport to the vacuole of heterologously expressed mung bean 8S globulin occurs in seed but not in vegetative tissues. J Exp Bot 64:1587–1601

Zienkiewicz A, Jimenez-Lopez JC, Zienkiewicz K, Alché JD, Rodríguez-García MI (2011a) Development of the cotyledon cells during olive (*Olea europaea* L.) in vitro seed germination and seedling growth. Protoplasma 248:51–765

Zienkiewicz A, Zienkiewicz K, Ben Ali S, Castro AJ, Rodríguez-García MI, Alché JD (2011b) Evaluation of the in vitro digestibility of seed storage proteins 11S-type in olive. In: Fundación del Olivar (Ed.), Actas del XV Simposium Científico-Técnico EXPOLIVA 2011. ISBN:978-84-938900-0-1

Zienkiewicz A, Zienkiewicz K, Rejón JD, Alché JD, Castro AJ, Rodríguez-García MI (2014) Olive seed protein bodies store degrading enzymes involved in mobilization of oil bodies. J Exp Bot 65:103–115